Influence of the vorticity-scalar correlation on mixing

Xi-Yuan Yin [1], Wesley Agoua, [1] Tong Wu [1,2] and Wouter J. T. Bos [1]
[1] *CNRS, Ecole Centrale de Lyon, INSA Lyon, Université Claude Bernard Lyon 1, LMFA, UMR5509, 69130 Écully, France*
[2] *Theoretical Physics I, University of Bayreuth, 95447 Bayreuth, Germany*

(Received 26 February 2024; accepted 20 September 2024; published 18 October 2024)

We investigate the role of the correlation between a scalar quantity and the vorticity in two-dimensional mixing at infinite Péclet number. We assess, using a diffusivity-independent mixing norm, the dynamics of both Galerkin-truncated ensembles and freely evolving two-dimensional scalar mixing. Both statistical mechanics and numerical experiments show how the mixing rate is attenuated when vorticity and scalar are initially correlated. Since the vorticity is shown to be a poorly mixing scalar, the results suggest that, in general, mixing can be enhanced by minimizing the correlation between vorticity and passive scalar.

DOI: 10.1103/PhysRevFluids.9.104502

I. INTRODUCTION

The present investigation considers the mixing (or stirring) of a passive scalar. The scalar can represent temperature fluctuations, pollutants, or any other passively advected quantity. The propension of a given flow to mix is determined by the dimensionality of space, the properties of the velocity field and of the scalar, the boundary conditions, the type of stirring, and initial conditions. We discuss these different features for the special case of two dimensions, considering an incompressible fluid, advecting a passive scalar.

The influence of boundary conditions is clearly very important, as shown by Raynal and Gence [1], comparing chaotic mixing in periodic and unbounded domains. Chaotic mixing in wall-bounded domains was considered by Gouillart *et al.* [2,3], where the presence of unmixed fluid near solid walls was shown to slow down the mixing. In turbulent flows, the generation of enstrophy near the walls was shown, on the contrary, to enhance mixing [4]. In the present case we will focus on the simplest, academic case of periodic boundary conditions, avoiding thereby the issues related to the influence of solid walls.

The stirring protocol is another important factor that we will omit from our analysis. Indeed, to obtain efficient mixing, the stirring protocol can be optimized under constraints [5,6]. We will let the flow freely evolve from initial conditions, in which case the precise type of the initial conditions will affect the mixing [7,8]. In particular the typical size of the initial scalar compared to the typical velocity length scales, or domain size, are important factors [9,10]. Moreover, the study of strange eigenmodes reveals the existence of scalar fields of slowest decay, which attract the long-time evolution of general initial scalar distributions [11,12], so that the rate of decay of scalar variance is still sensitive to initial conditions. Again, to keep the description as general as possible, we will consider random initial velocity and scalar fields. These fields are constituted by random Fourier modes with a prescribed energy spectrum for the velocity field, and analogously, a prescribed variance spectrum for the scalar quantity.

We have at this point simplified and specified the flow, the boundary conditions, omitted stirring, and prescribed random initial conditions. The problem is then determined, except for one point: To what extent the initial velocity and scalar fields are correlated? The influence of this initial

 ©2024 American Physical Society

correlation, more specifically the vorticity-scalar correlation, is the main subject of this study. This question has received little attention [13–15] and only a very partial understanding of the influence of the scalar-vorticity correlation on mixing exists. The question whether such an initial correlation is beneficial or, on the contrary, detrimental for mixing has not been answered.

In this work, we combine statistical mechanics and numerical simulations to better understand the influence of this correlation. In Sec. II we will show how any scalar field admits a decomposition into a correlated and an uncorrelated part. In the case of full correlation, the scalar is the same as the vorticity and is no longer passive. This decomposition allows us to use known results from equilibrium statistical mechanics to describe the mixing. We employ two numerical approaches to study this problem. In Sec. III, we present the theoretical predictions for a Galerkin truncated system and make assessments using pseudospectral numerical simulations. Equilibrium statistical mechanics applied to a truncated set of Fourier modes does not necessarily give an accurate description of the nontruncated system. Indeed, transported fields are well described by Lagrangian propagators [16]. This property was successfully used in Refs. [17,18] to study the influence of forcing in the mixing of active scalars versus passive ones. The Lagrangian structure of the equations is not retained in Eulerian discretizations such as Fourier-Galerkin methods, therefore, we use in Sec. IV a recently developed numerical method, called the characteristic mapping method (CMM) [19,20] , to assess the mixing of the full, nontruncated, system. Section V concludes this article and proposes potential future studies.

II. GOVERNING EQUATIONS AND CONSTANTS OF MOTION

We consider the advection of a passive scalar field $\phi(\boldsymbol{x}, t)$ in a two-dimensional (2D) periodic box Ω. The scalar is transported by a two-dimensional incompressible and inviscid flow whose velocity field $\boldsymbol{u}(\boldsymbol{x}, t)$ is described by the Euler equations. The curl of the velocity, or vorticity, $\omega(\boldsymbol{x}, t) = \nabla \times \boldsymbol{u}(\boldsymbol{x}, t)$ evolves according to

$$(\partial_t + \boldsymbol{u} \cdot \nabla)\omega = 0, \tag{1a}$$

$$\boldsymbol{u} = -\nabla \times \Delta^{-1}\omega, \tag{1b}$$

where the velocity can be recovered from the vorticity by the Biot-Savart relation Eq. (1b). The initial condition is $\omega(\boldsymbol{x}, 0) = \omega_0(\boldsymbol{x})$.

The linear advection equation under the velocity field $\boldsymbol{u}$ then describes the evolution of the scalar ϕ:

$$(\partial_t + \boldsymbol{u} \cdot \nabla)\phi = 0, \tag{2}$$

with $\phi(\boldsymbol{x}, 0) = \phi_0(\boldsymbol{x})$. As we wrote above, we consider a general case where the initial velocity and scalar field $\omega_0(\boldsymbol{x})$, $\phi_0(\boldsymbol{x})$ are random. The investigation of more specific initial conditions is left for further research.

The quadratic invariants, or constants of motion, of a two-dimensional Euler velocity field are

$$E = \int |\boldsymbol{u}|^2 d\boldsymbol{x}, \quad W = \int \omega^2 d\boldsymbol{x}. \tag{3}$$

The energy E and enstrophy W characterize the velocity field. One can define a typical wave number

$$k_\omega = \sqrt{W/E}. \tag{4}$$

This wave number characterizes the typical lengthscale of the velocity field. In the absence of sources and sinks, it remains constant, since W and E are conserved. The scalar field is also characterized by two invariants

$$S = \int \phi^2 d\boldsymbol{x}, \quad Q = \int \omega\phi d\boldsymbol{x}. \tag{5}$$

Whereas the variance S is determined by the scalar field only, the last quantity Q measures the correlation between the scalar and the vorticity field. The quantity Q is, like the other invariants, conserved in the absence of sources or sinks, so that its initial correlation persists throughout the evolution of the system.

Two-dimensional turbulence contains an infinite number of additional invariants, Casimirs of the form $\int f(\omega)d\boldsymbol{x}$. The choice to focus only on the four quantities E, W, S, Q is theoretically supported by the fact that in the Galerkin truncated system that we will consider first, they are the only surviving constants of motion, conserved, triad-by-triad by the nonlinear and advection terms [21,22]. The truncated system allows us to use a statistical mechanical approach in Sec. III, however since we ignore nearly all Casimirs, the investigation can be further refined. The Casimirs are a result of the conservative structure of the system which transport scalars along Lagrangian propagators. Therefore, we attempt to partially refine the study using a relabeling-based numerical method in Sec. IV.

Regardless of truncation, it remains in all cases that the vorticity-scalar correlation is an invariant of the system. Rescaling by the root-mean-square values, we define the relative correlation:

$$h = Q/\sqrt{SW}, \tag{6}$$

a quantity which is constrained by the bounds $0 \leqslant h \leqslant 1$. Our goal is to measure and understand the influence of h on mixing.

The passive scalar and the vorticity share the same evolution equations (2), (1). The difference is that the vorticity is related to the velocity by Eq. (1b). Since the evolution equation is identical, we can decompose the scalar into a correlated part which is proportional to the vorticity and an uncorrelated part ϕ':

$$\phi(\boldsymbol{x}, t) = (h\sqrt{S/W})\omega(\boldsymbol{x}, t) + \phi'(\boldsymbol{x}, t), \tag{7}$$

with the following relations

$$\int \phi'\omega d\boldsymbol{x} = 0 \quad \text{and} \quad S' \equiv \int \phi'^2 d\boldsymbol{x} = S(1 - h^2). \tag{8}$$

The quantities S and S' are independently conserved. The decomposition of the scalar Eq. (7) allows to simplify the problem and to formulate predictions for the statistical mechanics of the scalar using known results only. Indeed, the evolution of ϕ' to a statistical equilibrium state is governed by one invariant, S'. The evolution of the correlated part will be fully determined by the evolution of ω, since h is constant. Therefore, if $h = 1$, the problem of the mixing of the passive scalar becomes equivalent to the advection of the vorticity.

Before turning to the statistical description of mixing, we need to clarify how we measure mixing. The eventual fate of a scalar in a realistic flow is determined by diffusion. At sufficiently small values of the diffusivity, the mixing is piloted by the stretching and folding of the large-scale scalar structures. In the present investigation we will not consider the effect of diffusion and we will use the term mixing to denote the effect of the advection term on the scalar field. Note that sometimes the separate effect of advection is called stirring to distinguish it from the effect of diffusion.

We want thus to measure the mixing independently of the values of diffusion (and viscosity). We use a mixing norm previously introduced in the study of optimal mixing [23] (see also Ref. [24]). This measure is a function of the inverse gradient $|\nabla^{-1}\phi|$; its value is representative of the importance of the large scales of ϕ. We introduce a characteristic wave number

$$k_\phi = \sqrt{\frac{\int \phi^2 d\boldsymbol{x}}{\int |\nabla^{-1}\phi|^2 d\boldsymbol{x}}}. \tag{9}$$

An increase of this characteristic wave number indicates that the scalar is on average transported towards smaller scales. Typically this implies that the flow is mixing, since the eventual scalar dissipation in a realistic flow is taking place at the small scales (or large wave numbers). We also note that in a periodic domain, for scalar ϕ, one can check by Parseval's identity that $\int |\nabla^{-1}\phi|^2 d\boldsymbol{x} = \sum_{\boldsymbol{k}} k^{-2}|\hat{\phi}(\boldsymbol{k})|^2 = \int |-\nabla \times \Delta^{-1}\phi|^2 d\boldsymbol{x}$ so that the typical wave number k_ω [introduced in Eq. (4)] is the ratio of the L^2 to H^{-1} seminorms for ω, and k_ϕ is the same ratio for ϕ.

There is currently no consensus on the optimal choice of a mixing norm [23–27]. The present definition of a typical wave number k_ϕ allows, by introducing the quantity $\sum_{\boldsymbol{k}} k^{-n}|\hat{\phi}(\boldsymbol{k})|^2$ with $n = 2$, to focus on the evolution of the large scales of the scalar field. Larger values of n would further increase the relative weight of the large scales in the definition of k_ϕ. The advantage of $n = 2$ is that the limit where $\phi = \omega$ corresponds to the case where $k_\phi = k_\omega =$ constant (since the Euler equations conserve both energy and enstrophy).

One might argue that the vorticity mixes and that a constant value of k_ϕ does not correctly reflect this. We note, however, that the mixing scale k_ϕ is not intended as an absolute measure for mixing, but a relative one: comparing the value and evolution of k_ϕ for different scalar initial conditions allows to determine which field is subjected to the strongest mixing under a given flow. We do not further attempt to find the perfect measure for mixing and we will use expression (9). We anticipate that using this definition, for most of the results in Sec. III and all the results Sec. IV, it turns out that the reference case where $\phi = \omega$ is essentially the worst mixing scalar.

In the following, we will investigate the evolution of k_ϕ for given values of h and k_ω. We will start by deriving a theoretical prediction.

III. THEORETICAL PREDICTIONS AND NUMERICAL VERIFICATION FOR MIXING IN THE GALERKIN TRUNCATED SYSTEM

We consider that the velocity and scalar excitation are projected on a finite number of Fourier modes in two-dimensional Fourier space. The smallest and largest wave number are k_0, k_1, respectively. The evolution equations are also restricted to keep the excitation confined on these modes. The scalar variance is then obtained by

$$\int_{k_0}^{k_1} E_\phi(k)dk = S. \tag{10}$$

And a similar expression relates $E_{\phi'}(k)$ and S'. In such a setup, the equilibrium solution of the uncorrelated passive scalar is given by the equipartition solution

$$E_{\phi'}(k, t = \infty) = c_\phi k, \tag{11}$$

where $c_\phi = 2S'/(k_1^2 - k_0^2)$ (see, for instance, Ref. [28]). This simple expression describes the equilibrium spectrum associated with ϕ'. The correlated part is fully determined by the vorticity field and its dynamics is determined by both the kinetic energy and the enstrophy. Indeed, the energy spectrum determines both quantities according to

$$\int_{k_0}^{k_1} E(k)dk = E, \quad \int_{k_0}^{k_1} k^2 E(k)dk = W. \tag{12}$$

For the scalar spectrum we have therefore

$$E_\phi(k, t) = E_{\phi'}(k, t) + h^2 \frac{S}{W} k^2 E(k, t). \tag{13}$$

To verify this relation, we carry out numerical simulations of the system. Standard Cartesian pseudospectral solvers are the ideal tools to verify the present predictions of equilibrium statistical mechanics, since these methods are based on a Galerkin truncation [29] and since they are known to correctly conserve the invariants of the system. We use the two-dimensional code Ghost [30], based on a vorticity-streamfunction formulation and second-order time integration. We start from a Gaussian-shaped initial spectrum $E(k, 0) \sim \exp(-b(k - k_L)^2)$, with random Fourier phases and $k_L = 4$ and $b = 0.125$, setting the total energy at 1 and enstrophy at approximately 28, i.e., $k_\omega \approx 5.3$.

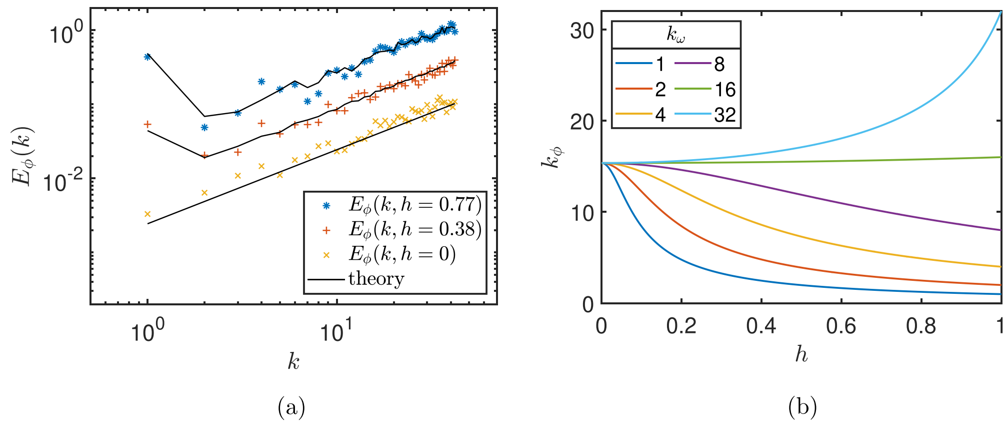

FIG. 1. Results and predictions for equilibrium ensembles of the Galerkin truncated system. The wave number range is confined to $k \in [1, 42]$. (a) DNS results for the equilibrium spectra of the scalar variance $E_\phi(k)$. Theory predicts a spectrum of $h^2(S/W)k^2E(k) + c_\phi k$ from Eq. (13). For clarity of the image, the $h = 0.38$ and $h = 0.77$ data are shifted up by a half and full decade, respectively. (b) Influence of the relative correlation h on the mixing scale k_ϕ predicted from Eq. (14). Results are shown for different values of the characteristic velocity scale k_ω.

We plot in Fig. 1(a) the spectra $E_\phi(k, t = t_\infty)$ and the estimate Eq. (13), with $E_{\phi'}(k) = c_\phi k$. For each value of $h(t = 0)$ a different statistical realization of the initial conditions for $E(k, 0)$ is used. The time t_∞ is determined by running the simulations for $t \approx 8000 t_*$, with $t_* = W^{-1/2}$, a time sufficient for the statistics to converge to a statistical equilibrium. It is observed that the predicted spectrum is well approached by the theoretical estimate. We can then use this theoretical estimate of the scalar spectrum to compute analytically the mixing scale k_ϕ.

Using Parseval's relation between the mixing norm and the scalar spectrum $\int |\nabla^{-1}\phi|^2 d\boldsymbol{x} = \int_{k_0}^{k_1} k^{-2}E_\phi(k)dk$, we find, after some elementary manipulation for the mixing scale,

$$k_\phi = \left[h^2 k_\omega^{-2} + (1 - h^2)k_{\phi'}^{-2}\right]^{-1/2}, \tag{14}$$

where $k_{\phi'} = ((k_1^2 - k_0^2)/(2\ln(k_1/k_0)))^{1/2}$. The two limits of these expression are, for $k_\phi(h = 1) = k_\omega$, where the mixing scale is fully determined by the typical velocity length scale. And for the uncorrelated case we have $k_\phi(h = 0) = k_{\phi'}$.

Expression (14) is plotted for fixed resolution (or $k_{\phi'}$) in Fig. 1(b). We see there that the influence of finite h is for most cases deleterious, i.e., k_ϕ is a decreasing function of h. Only for large initial k_ω this effect is not observed. Nevertheless, this latter case corresponds to initial conditions where the initial scalar field is concentrated at scales much larger than the excited velocity scales. In realistic flows this will lead to very slow mixing. The reason that statistical mechanics predict enhanced mixing for this case is that only final states are predicted, irrespective of the time it takes to reach such an equilibrium state. This constitutes the limit of equilibrium-statistical mechanics to predict realistic flows and we will therefore in the following use numerical simulations to understand the dynamics of the full, nontruncated system.

IV. SIMULATIONS OF SCALAR MIXING BY THE EULER EQUATIONS

What we can retain from the results of equilibrium statistical mechanics is that it indicates a tendency of less efficient mixing when the vorticity-scalar correlation is strong. The worst mixing is attained when the velocity scale is largest, $k_\omega/k_0 \approx 1$. We note that this is a relevant case, since two-dimensional flows are often dominated by space-filling structures.

We will assess now if, as suggested by statistical mechanics, mixing is reduced when $h \neq 0$, dynamically, when the system is not Galerkin truncated. Simulating the evolution of vorticity and the mixing of a scalar without the influence of viscosity and diffusion is numerically challenging. Nevertheless, recent advances in numerical analysis have led to the development of a numerical method allowing to compute, in a precise and efficient way, exactly this evolution. The method we therefore apply is the characteristic mapping method (CMM [19,20]), a method which, instead of advancing the Eulerian fields such as vorticity and velocity, evolves the inverse flow map $\boldsymbol{X}_B$. This map, also called back-to-label map, is given by

$$(\partial_t + \boldsymbol{u}\cdot\nabla)\boldsymbol{X}_B = 0, \tag{15a}$$

$$\boldsymbol{X}_B(\boldsymbol{x}, 0) = \boldsymbol{x}, \tag{15b}$$

and maps time t Eulerian positions $\boldsymbol{x}$ to the initial position of the corresponding Lagrangian tracer. One can check that for any advected quantity ϕ solving Eq. (2), the time t solution can be expressed as a relabeling of the initial condition via

$$\phi(\boldsymbol{x}, t) = \phi_0(\boldsymbol{X}_B(\boldsymbol{x}, t)). \tag{16}$$

These types of discretization methods act through direct pullback of the initial condition and preserve the Lagrangian propagation structure of the advection equation so that all fields are transported by the same Lagrangian propagators.

An immediate advantage is that once the flow map is determined for a given flow, it allows to determine directly the scalar field $\phi(\boldsymbol{x}, t)$ for all possible initial conditions $\phi_0(\boldsymbol{x})$. Furthermore, the solution of this advection is not frequency truncated and solves the nondiffusive advection. The Casimirs and invariants of the system are naturally conserved so that we can compare the statistical predictions for the truncated system with the long-time solutions of the nontruncated one.

Here we remark that, in the presence of viscosity and diffusion, propagators have stochastic trajectories. In typical turbulent flows, due to the roughness of the limiting velocity, propagators remain stochastic in the limit of zero viscosity, resulting in anomalous diffusion of advected scalars (see Ref. [16] and references therein). We note that for the case studied here, the solution of the incompressible Euler equations in two dimensions with smooth initial condition remains smooth for all times, therefore trajectories are deterministic and propagators are Dirac measures. This is in contrast to the finite viscosity and diffusivity case where stochasticity of the Lagrangian propagators must be taken into account [17,18].

For the tests performed here we start from an initial velocity field given by an enstrophy spectrum concentrated around k_ω with random phases and normalized to unit kinetic energy. The initial scalar spectrum is defined by the bump function with $k_\phi \approx 3.3$. The evolution of the energy spectrum and the scalar spectrum are shown in Fig. 2(a) for a range of correlation values. We see that as correlation decreases, more scalar energy is moved towards the small scales, indicating a better mixing.

We quantify the extent of the mixing enhancement using the mixing norm of ϕ. Define the enhancement

$$M(\phi, t) = \frac{k_{\phi(t)}}{k_{\phi(0)}} = \sqrt{\frac{\int |\nabla^{-1}\phi(0)|^2 d\boldsymbol{x}}{\int |\nabla^{-1}\phi(t)|^2 d\boldsymbol{x}}}, \tag{17}$$

where the second equality is obtained from the fact that $\int \phi^2 d\boldsymbol{x}$ is a conserved quantity. The enhancement number $M(\phi, t)$ measures the relative increase of the typical wave number in time due to transport by the fluid. The essential difference with the results of equilibrium statistical mechanics is that the enhancement measure $M(\phi, t)$ takes into account the initial conditions, whereas equilibrium statistical mechanics only gives information on the final state, irrespective of initial conditions. We note that in the $h = 1$ fully correlated case, $\phi = (Q/W)\omega$, in which case $k_\phi = k_\omega = \sqrt{W/E}$, which is a constant of motion, and hence $M(\phi, t)$ must remain 1.

To test the influence of the scalar-vorticity correlation on the mixing enhancement, we perform the scalar advection using three flows obtained from the Euler equations where the typical wave

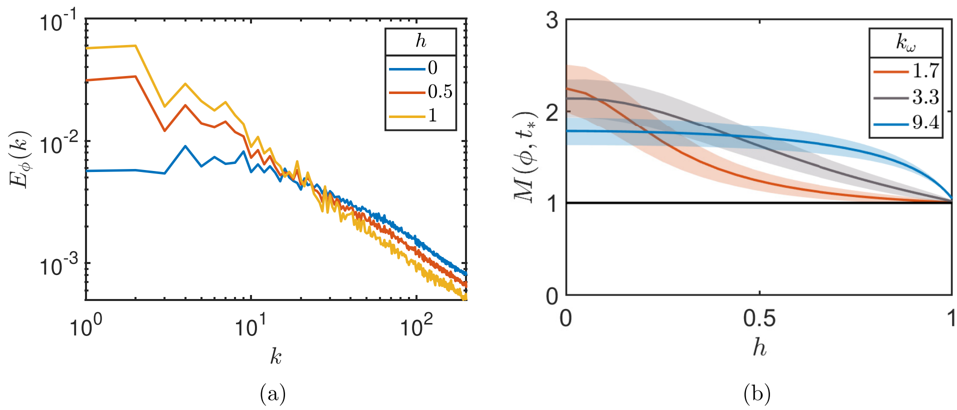

FIG. 2. Results from computations using the Characteristic Mapping Method (CMM). Panel (a) shows the final time-scalar spectra for various correlation values, with initial conditions $k_{\phi(0)} \approx k_{\omega(0)} \approx 3.3$. Panel (b) shows the mixing enhancement $M(\phi, t_*)$ as function of the scalar-vorticity correlation when transported by various flows for a given amount of time. The average enhancement over a sample of 30 scalars is shown in full line, the shaded area covers one standard deviation.

number k_ω is approximately 1.7, 3.3, and 9.4 respectively. We generate for each flow a sample of 30 initial conditions ϕ_0' of random phase and bump function spectrum such that ϕ_0' are fully decorrelated from the vorticity ω_0 and $k_{\phi_0'} \approx 3.3$. Each ϕ' correspond to the $h = 0$ case, and together with ω, we generate a family of initial conditions ϕ ranging from $h = 0$ to $h = 1$ and whose initial characteristic length k_{ϕ_0} range from $k_{\phi_0'}$ to k_ω. This effectively tests for the mixing enhancement generated by a flow which moves at larger, equal, and smaller spatial scales than the advected quantity. Figure 2(b) shows the results from our tests and a visual comparison between low and high correlation scalar fields before and after advection is shown in Fig. 3. The time t at which the enhancement is assessed is fixed at $t \approx 20t_*$ with $t_* = W^{-1/2}$ as to normalize the average turnover over the three flows. The same tests can be performed by instead scaling t with $E^{-1/2}$, but have similar results due to the scaling symmetry of the Euler equations. In all cases, we observe that the mixing enhancement is a monotonously decreasing function of the correlation h. However, it seems that the sensitivity of the mixing enhancement to variations of the correlation is not uniform. For cases where the flow's typical wave number k_ω is larger than that of the initial scalar, the correlation affects the mixing less, possibly due to scale separation. This was also suggested by the statistical prediction in Fig. 1(b).

Although the systems examined in Secs. III and IV are different, the results we obtain are similar: the correlation of the passive scalar with the vorticity field at initial time is, in general, detrimental to mixing. We think that this agreement may be caused by the fact that for two-dimensional flow the large-scale dynamics of the Galerkin truncated equations approximate well to that of the Euler equations at large enough resolution. Consequently, the statistical predictions in the truncated finite-dimensional system remain relevant for the full system.

V. CONCLUSION

The fact that initial velocity conditions are important for the efficiency of mixing is not surprising. However, the fact that for a given random scalar field and a given random velocity field, fixing E, W, S, the mixing can be as dramatically affected by the value of Q as observed in Fig. 2 is something which might not have been expected from the outset. Indeed, the mixing scale for $h = 1$ remains constant, while for the fully uncorrelated case the mixing enhancement, for all our tests, is consistently higher, typically by more than a factor of 2. We were not able to verify mathematically

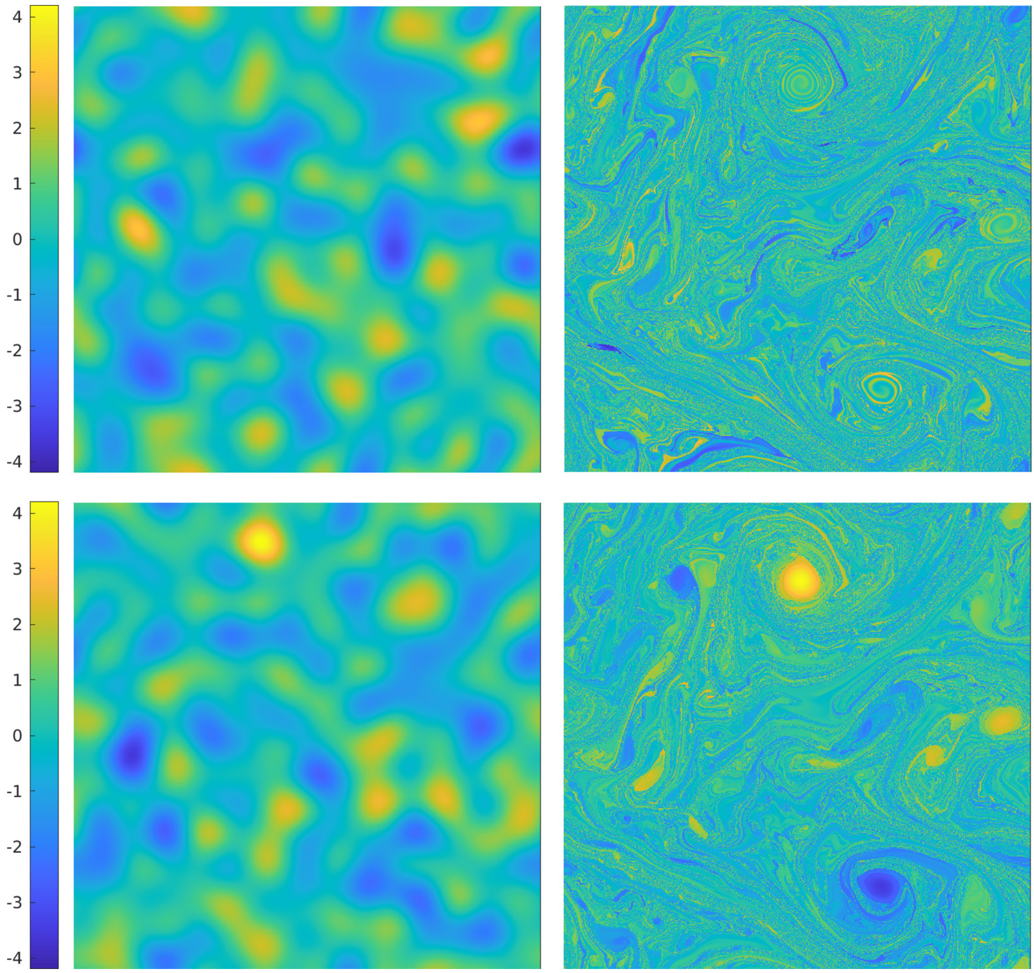

FIG. 3. Results from CMM computations. Panels (a) and (b) show the initial- and final-time scalar fields for the $h = 0$ and $h = 1$ cases, respectively.

if the vorticity field is the least mixed scalar, however our numerical experiments and analysis (see Appendix) suggest that, in general, it is a badly mixed scalar.

In the definition of the mixing scale and the invariants of the system, we have not explicitly assumed that the system is turbulent. We do therefore think that these ideas can be applied to nonturbulent systems as well. A practical implication of the present insights is that, in optimization problems (e.g., Refs. [5,25,31]), the constraint of minimizing the correlation between scalar and vorticity might be a powerful way to approach the optimal mixing regime in both turbulent and nonturbulent flows.

ACKNOWLEDGMENT

All DNS simulations were carried out using the facilities of the PMCS2I (École Centrale de Lyon). The authors acknowledge funding from the Agence Nationale de la Recherche (ANR), project CM2E, Grant No. ANR-20-CE46-0010-01.

APPENDIX: WHAT IS THE WORST-MIXING SCALAR IN TWO-DIMENSIONAL EULER FLOW?

Consider any random scalar field θ, we try to find the most- or least-mixed scalar field in the plane spanned by ω and θ, with the objective of understanding what inhibits mixing and whether the vorticity field is the least-mixed scalar in 2D. Up to rescaling, all scalar fields ϕ spanned by combinations of ω and θ can be written in the form

$$\phi = \cos(\alpha)\theta + \sin(\alpha)\omega. \tag{A1}$$

For this part, we do not assume that θ and ω are uncorrelated, only that $\theta \neq \omega$.

The problem is then reduced to extremizing the mixing enhancement $M(\phi, t)$ by choice of α. We note that by conservation of $\langle \phi^2(t) \rangle$ in time from the advection, we have

$$M^2(\phi, t) = \frac{\int |\nabla^{-1}\phi(0)|^2 d\boldsymbol{x}}{\int |\nabla^{-1}\phi(t)|^2 d\boldsymbol{x}}. \tag{A2}$$

Denote for convenience $m_\phi = \int |\nabla^{-1}\phi|^2 d\boldsymbol{x}$, $m_\theta = \int |\nabla^{-1}\theta|^2 d\boldsymbol{x}$, $m_\omega = \int |\nabla^{-1}\omega|^2 d\boldsymbol{x} = 2E$, and $m_c = \int \nabla^{-1}\theta \cdot \nabla^{-1}\omega d\boldsymbol{x} = \langle \theta\psi \rangle$, where $\psi = \Delta^{-1}\omega$ is the stream function. We have that

$$\int |\nabla^{-1}\phi|^2 d\boldsymbol{x} = \cos^2(\alpha) m_\theta + \sin^2(\alpha) m_\omega + 2\cos(\alpha)\sin(\alpha) m_c. \tag{A3}$$

This allows us to write a closed-form formula for $M(\phi, t)$ in terms of α, $m_\theta(0)$, $m_\theta(t)$, m_ω, $m_c(0)$, and $m_c(t)$. Since energy is conserved, we do not write the time dependence of m_ω.

In order to find critical points of the mixing enhancement, we evaluate the sign of the derivative of $M^2(\phi, t)$ with respect to α. This is determined by the sign of

$$\begin{aligned} m_\phi^2(t)\partial_\alpha M^2(\phi, t) &= m_\phi(t)\partial_\alpha m_\phi(0) - m_\phi(0)\partial_\alpha m_\phi(t) \\ &= m_\phi(t)(\sin(2\alpha)(m_\omega(0) - m_\theta(0)) + 2\cos(2\alpha)m_c(0)) \\ &\quad - m_\phi(0)(\sin(2\alpha)(m_\omega(t) - m_\theta(t)) + 2\cos(2\alpha)m_c(t)). \end{aligned} \tag{A4}$$

For the least-mixed scalar on the ω-θ plane, as measured by the H^{-1} mix norm, the above α derivative should be zero. Since we took θ arbitrarily, unless ω is already the least-mixed scalar, we may assume without loss of generality that the least mixing is achieved by θ, i.e., at $\alpha = 0$, with $\phi|_{\alpha=0} = \theta$. The vanishing derivative condition then gives

$$0 = m_\theta(t)m_c(0) - m_\theta(0)m_c(t) \quad \text{or} \quad M(\theta, t) = \frac{m_\theta(0)}{m_\theta(t)} = \frac{m_c(0)}{m_c(t)}, \tag{A5}$$

that is, the mixing enhancement of the most- and least-mixed scalar is given by its correlation with the stream function.

Since we assumed that the mixing of θ is worse than that of ω, we have $M(\theta, t) \leqslant M(\omega, t) = 1$, so that the condition for the least-mixed scalar to be less mixed than the vorticity is

$$\langle \theta(0)\psi(0) \rangle \leqslant \langle \theta(t)\psi(t) \rangle, \tag{A6}$$

that is, the correlation of the scalar field with the stream function is stronger for larger times.

Although the initial stream function is determined by the initial conditions of the flow, we generally observe that in flows governed by the 2D incompressible Euler equations, the long-time behavior tends towards a quasisteady state where the vorticity field and the stream function satisfy a functional relation. This behavior has been observed extensively in DNS and was predicted theoretically [32–35]. This supports the observation that, in general, correlation with the vorticity field inhibits mixing as vorticity is a decent predictor of the stream function for large times. However, this does not necessarily mean that the vorticity field is the least-mixed scalar on any θ-ω plane. The question of finding the most- and least-mixed scalar field in the infinite-time asymptotics still remains open and subject to further investigation.

[1] F. Raynal and J.-N. Gence, Energy saving in chaotic laminar mixing, Int. J. Heat Mass Transf. **40**, 3267 (1997).

[2] E. Gouillart, N. Kuncio, O. Dauchot, B. Dubrulle, S. Roux, and J.-L. Thiffeault, Walls inhibit chaotic mixing, Phys. Rev. Lett. **99**, 114501 (2007).

[3] E. Gouillart, O. Dauchot, B. Dubrulle, S. Roux, and J. L. Thiffeault, Slow decay of concentration variance due to no-slip walls in chaotic mixing, Phys. Rev. E **78**, 026211 (2008).

[4] B. Kadoch, W. J. T. Bos, and K. Schneider, Efficiency of laminar and turbulent mixing in wall-bounded flows, Phys. Rev. E **101**, 043104 (2020).

[5] D. P. G. Foures, C. P. Caulfield, and P. J. Schmid, Optimal mixing in two-dimensional plane Poiseuille flow at finite Péclet number, J. Fluid Mech. **748**, 241 (2014).

[6] M. F. Eggl and P. J. Schmid, Mixing enhancement in binary fluids using optimised stirring strategies, J. Fluid Mech. **899**, A24 (2020).

[7] M. Farazmand, Optimal initial condition of passive tracers for their maximal mixing in finite time, Phys. Rev. Fluids **2**, 054601 (2017).

[8] M. Singh, E. Germaine, L. Mydlarski, and L. Cortelezzi, Dependence of scalar mixing on initial conditions in turbulent channel flow, Phys. Rev. Fluids **8**, 124605 (2023).

[9] A. A. Schekochihin, P. H. Haynes, and S. C. Cowley, Diffusion of passive scalar in a finite-scale random flow, Phys. Rev. E **70**, 046304 (2004).

[10] P. H. Haynes and J. Vanneste, What controls the decay of passive scalars in smooth flows? Phys. Fluids **17**, 097103 (2005).

[11] W. Liu and G. Haller, Strange eigenmodes and decay of variance in the mixing of diffusive tracers, Physica D **188**, 1 (2004).

[12] J. Sukhatme and R. T. Pierrehumbert, Decay of passive scalars under the action of single scale smooth velocity fields in bounded two-dimensional domains: From non-self-similar probability distribution functions to self-similar eigenmodes, Phys. Rev. E **66**, 056302 (2002).

[13] G. Holloway and S. S. Kristmannsson, Stirring and transport of tracer fields by geostrophic turbulence, J. Fluid Mech. **141**, 27 (1984).

[14] M. Lesieur and J. R. Herring, Diffusion of a passive scalar in two-dimensional turbulence, J. Fluid Mech. **161**, 77 (1985).

[15] M. Linkmann, M. Buzzicotti, and L. Biferale, Nonuniversal behaviour of helical two-dimensional three-component turbulence, Eur. Phys. J. E **41**, 4 (2018).

[16] G. Falkovich, K. Gawedzki, and M. Vergassola, Particles and fields in fluid turbulence, Rev. Mod. Phys. **73**, 913 (2001).

[17] A. Celani, M. Cencini, A. Mazzino, and M. Vergassola, Active versus passive scalar turbulence, Phys. Rev. Lett. **89**, 234502 (2002).

[18] A. Celani, M. Cencini, A. Mazzino, and M. Vergassola, Active and passive fields face to face, New J. Phys. **6**, 72 (2004).

[19] O. Mercier, X.-Y. Yin, and J.-C. Nave, The characteristic mapping method for the linear advection of arbitrary sets, SIAM J. Sci. Comput. **42**, A1663 (2020).

[20] X.-Y. Yin, O. Mercier, B. Yadav, K. Schneider, and J.-C. Nave, A characteristic mapping method for the two-dimensional incompressible Euler equations, J. Comput. Phys. **424**, 109781 (2021).

[21] D. Fyfe, D. Montgomery, and G. Joyce, Dissipative, forced turbulence in two-dimensional magnetohydrodynamics, J. Plasma Phys. **17**, 369 (1977).

[22] R. H. Kraichnan and D. Montgomery, Two-dimensional turbulence, Rep. Prog. Phys. **43**, 547 (1980).

[23] G. Mathew, I. Mezić, and L. Petzold, A multiscale measure for mixing, Physica D **211**, 23 (2005).

[24] J.-L. Thiffeault, Using multiscale norms to quantify mixing and transport, Nonlinearity **25**, R1 (2012).

[25] Z. Lin, J.-L. Thiffeault, and C. R. Doering, Optimal stirring strategies for passive scalar mixing, J. Fluid Mech. **675**, 465 (2011).

[26] C. Heffernan and Colm-cille P. Caulfield, Robust and efficient identification of optimal mixing perturbations using proxy multiscale measures, Philos. Trans. R. Soc. A **380**, 20210026 (2022).

[27] M. C. Zelati, G. Crippa, G. Iyer, and A. L. Mazzucato, Mixing in incompressible flows: Transport, dissipation, and their interplay, Notices Amer. Math. Soc. **2024**, 593 (2024).

[28] C. E. Leith, Diffusion approximation for turbulent scalar fields, Phys. Fluids **11**, 1612 (1968).
[29] S. A. Orszag, Numerical methods for the simulation of turbulence, Phys. Fluids **12**, II-250 (1969).
[30] P. D. Mininni, D. Rosenberg, R. Reddy, and A. Pouquet, A hybrid MPI-OpenMP scheme for scalable parallel pseudospectral computations for fluid turbulence, Parallel Computing **37**, 316 (2011).
[31] E. Lunasin, Z. Lin, A. Novikov, A. Mazzucato, and C. R. Doering, Optimal mixing and optimal stirring for fixed energy, fixed power, or fixed palenstrophy flows, J. Math. Phys. **53**, 115611 (2012).
[32] G. Joyce and D. Montgomery, Negative temperature states for the two-dimensional guiding-centre plasma, J. Plasma Phys. **10**, 107 (1973).
[33] D. Montgomery and G. Joyce, Statistical mechanics of "negative temperature" states, Phys. Fluids **17**, 1139 (1974).
[34] J. Miller, Statistical mechanics of Euler equations in two dimensions, Phys. Rev. Lett. **65**, 2137 (1990).
[35] R. Robert and J. Sommeria, Statistical equilibrium states for two-dimensional flows, J. Fluid Mech. **229**, 291 (1991).